VERSITA

Acta Geophysica
vol. 61, no. 4, Aug. 2013, pp. 775-807
DOI: 10.2478/s11600-013-0130-4

Dedicated to the memory of Minoru M. Freund

Earthquake Forewarning – A Multidisciplinary Challenge from the Ground up to Space

Friedemann FREUND

NASA Ames Research Center, Moffett Field, CA, USA
e-mail: friedemann.t.freund@nasa.gov
Department of Physics, San Jose State University, San Jose, CA, USA
Carl Sagan Center (CSC), SETI Institute, Mountain View, CA, USA

A b s t r a c t

Most destructive earthquakes nucleate at between 5-7 km and about 35-40 km depth. Before earthquakes, rocks are subjected to increasing stress. Not every stress increase leads to rupture. To understand pre-earthquake phenomena we note that igneous and high-grade metamorphic rocks contain defects which, upon stressing, release defect electrons in the oxygen anion sublattice, known as positive holes. These charge carriers are highly mobile, able to flow out of stressed rocks into surrounding unstressed rocks. They form electric currents, which emit electromagnetic radiation, sometimes in pulses, sometimes sustained. The arrival of positive holes at the ground-air interface can lead to air ionization, often exclusively positive. Ionized air rising upward can lead to cloud condensation. The upward flow of positive ions can lead to instabilities in the mesosphere, to mesospheric lightning, to changes in the Total Electron Content (TEC) at the lower edge of the ionosphere, and electric field turbulences. Advances in deciphering the earthquake process can only be achieved in a broadly multidisciplinary spirit.

Key words: pre-earthquake signals, peroxy defects, positive holes, air ionization, mesospheric lightning, ionospheric perturbations, Total Electron Content.

1. INTRODUCTION

For decades, even centuries, strange phenomena have been reported to become observable before major earthquakes. These pre-earthquake (pre-EQ) phenomena are non-seismic in nature. They are generally subtle and fleeting, sometimes distinct and strong, at other times seemingly absent. Often they seem not to be connectable to any known physical or chemical process, even outright incomprehensible. Non-seismic pre-EQ phenomena comprise local magnetic field variations, EM emissions from VIS through IR and GHz to ULF/ELF frequencies[1], excess radon emanation from the ground, changes in water chemistry, water condensation in the atmosphere leading to haze, fog or clouds, atmospheric gravity waves (AGW) rising up to the ionosphere, changes in the Total Electron Content (TEC) at the lower edge of the ionosphere, and even the most contentious all reported pre-EQ phenomena: unusual animal behavior.

In an earlier paper in *Acta Geophysica* entitled "Toward a unified solid state theory for pre-earthquake signals" (Freund 2010) I described a little known solid state discovery that has proven helpful in deciphering pre-EQ phenomena: metastable peroxy defects in minerals in igneous and high-grade metamorphic rocks, which release highly mobile electronic charge carriers, when the rocks are subjected to mechanical stress. Those charge carriers consist of defect electrons in the oxygen anion sublattice. Known as "positive holes", they are associated with energy states at the upper edge of the valence bands and have amazing properties.

In this report I'll review the basic elements of positive hole charge carriers, how there are introduced into the matrix of rock-forming minerals, and what their role is in generating pre-EQ signals. I'll focus on processes that can be traced back to the arrival of positive hole charge carriers at the ground-to-air interface – only a segment out of the multitude of pre-EQ signals. However, I'll also present new insight that has emerged since the publication of the earlier paper – insight, which has is leading to a better understanding of some old pre-EQ signals and to the anticipation of some new ones.

2. A FAMILY OF OVERLOOKED DEFECTS IN MINERALS

A large body of literature exists dealing with the oxidation or valence state of cations in various oxide and silicate minerals. The study how reduced or how oxidized transition metal cations are in different mineral phases, for instance Fe^{2+}/Fe^{3+}, is widely used to determine the redox conditions under

[1)] EM – electromagnetic, VIS – visible, IR – infrared, GHz – 10^9 Hz, ULF/ELF – 10 Hz to mHz to μHz.

which the rocks had formed and to reconstruct their cooling history. By contrast, oxygen anions are always tacitly assumed to be in the valence 2– except in the case of radiation defects in minerals, where oxygen anions in the valence 1– may occur, stable mostly or exclusively at cryogenic temperatures (Fukuchi 1996, Griscom 1990, Marfunin 1979). However, evidence accumulated over the course of more than 30 years suggests that oxygen in the valence 1– can exist and does exist in oxide materials and in silicate minerals of igneous and high-grade metamorphic rocks. The presence of O^-, albeit in a metastable state, is crucial for understanding electrical properties of rocks in the Earth crust down to about 35-40 km. They are also crucial for understanding a wide range of electrical phenomena linked to processes that occur in the Earth's crust prior to earthquakes.

2.1 How peroxy defects are introduced into minerals

MgO was the first oxide material for which it was shown that the valence of oxygen anions is not fixed at 2–, but can change to the higher oxidation state 1–. The solid state reaction studied at that time was the thermal decomposition of $Mg(OH)_2$ which – according to textbook knowledge – should simple produce MgO plus H_2O:

$$Mg(OH)_2 \Leftrightarrow MgO + H_2O \ . \tag{1a}$$

In reality the finely divided MgO formed as a decomposition product retains a relatively large concentration of residual OH^-:

$$Mg(OH)_2 \Leftrightarrow Mg_{1-\delta}(OH)_{2\delta}O_{1-2\delta} + 1 - \delta\ H_2O \ . \tag{1b}$$

Normally one would expect that, upon further heating to sufficiently high temperatures, this OH^-–rich MgO would split off additional H_2O and turn into stoichiometric MgO:

$$Mg_{1-\delta}(OH)_{2\delta}O_{1-2\delta} \Rightarrow MgO + \delta\ H_2O \ . \tag{1c}$$

However, the situation is not so simple. When $Mg(OH)_2$ is thermally decomposed to $MgO + H_2O$, it forms a dilute $MgO - H_2O$ solid solution, $Mg_{1-\delta}(OH)2\delta O_{1-2\delta}$. Even using ultrahigh purity materials, MgO with a cationic impurity level < 5 ppm, the $MgO - H_2O$ solid solution was found to release copious amounts of H_2, 10 000 ppm (Martens *et al*. 1976). Since Mg cations are fixed in the 2+ valence state, the only possibility for H^+ to be reduced to H_2 in such quantities was to concomitantly oxidize oxygen anions from their common valence 2– to the valence 1–.

$$Mg_{1-\delta}(OH)_{2\delta}O_{1-2\delta} \Rightarrow Mg_{1-\delta}O + \delta\ H_2 \ . \tag{1d}$$

Follow-on studies with MgO single crystals provided insight where in the MgO matrix this unusual reaction takes place: it involves OH^- pairs associated with Mg^{2+} vacancies that undergo a redox conversion during cooling, in the course of which the two OH^- protons become reduced to H, forming H_2, while the two hydroxyl O^{2-} become oxidized to O^-, forming a peroxy anion, O_2^{2-} (Batllo *et al*. 1991, Freund and Wengeler 1982).

Using the Kröger–Vinck point defect designation[2] we can write this solid state reaction as:

$$\left[\mathrm{OH}^{\bullet} V''_{\mathrm{Mg}}\, \mathrm{HO}^{\bullet}\right]^x \Leftrightarrow \left[\begin{matrix}\mathrm{O}^{\cdot\cdot}\\ \mathrm{O}\end{matrix} (\mathrm{H}_2)''_{\mathrm{Mg}}\right]^x . \qquad (2)$$

Being diffusively mobile the H_2 can transition from the Mg^{2+} vacancy site to an interstitial site:

$$\left[\begin{matrix}\mathrm{O}^{\cdot\cdot}\\ \mathrm{O}\end{matrix} (\mathrm{H}_2)''_{\mathrm{Mg}}\right]^x \Leftrightarrow \left[\begin{matrix}\mathrm{O}^{\cdot\cdot}\\ \mathrm{O}\end{matrix} V''_{\mathrm{Mg}}\right]^x + (\mathrm{H}_2)_i^x . \qquad (3)$$

Here the right side describes an Mg^{2+} vacancy chargewise compensated by a peroxy anion, O_2^{2-}. If the MgO crystals are very small (Martens *et al*. 1976), the H_2 can easily escape, thereby changing $Mg_{1-\delta}(H_2)_\delta O$ into $Mg_{1-\delta}O$. If $\delta << 1$, the cation-deficient $Mg_{1-\delta}O$ may also be written as MgO with excess of oxygen, $MgO_{1+\delta}$.

Pure MgO is intrinsically diamagnetic. Peroxy anions are also diamagnetic, but when their O^-–O^- bond breaks up, they turn paramagnetic. Magnetic susceptibility studies have provided valuable information about the temperature-induced peroxy break-up (Batllo *et al*. 1991). Electrical conductivity and dielectric polarization measurements provided information that, during break-up of the peroxy anions, highly mobile electronic charge carriers are released which affect the electrical properties of the MgO in dramatic ways (Freund *et al*. 1989, Kathrein and Freund 1983). These charge carriers are defect electrons in the O^{2-} sublattice, chemically O^- in a matrix of O^{2-}. They have been called positive holes and designated as $h^{\bullet}$ (Griscom 1990).

Peroxy links are known point defects in fused silica (Ricci *et al.* 2001). These peroxy links are probably introduced when O_3Si-O-SiO_3 bonds are hydrolyzed, first forming O_3Si-OH pairs, then undergoing the same type of

[2)] V stands for vacancy; subscripts identify the site (except for oxygen sites, where subscripts are omitted); superscript prime, dot, and x designate single negative, positive, and neutral charges, respectively, double prime and double dot designate double negative and positive charges; subscript i means interstitial; square brackets outline the essential parts of any given point defect.

redox conversion as OH^- pairs in the MgO matrix (Freund and Masuda 1991):

$$O_3Si\,/^{O}\backslash SiO_3 + H_2O \Leftrightarrow O_3Si\,/^{OH}{}_{HO}/SiO_3 \ , \tag{4a}$$

$$O_3Si\,/^{OH}{}_{HO}/SiO_3 \Leftrightarrow O_3Si\,/^{OO}\backslash SiO_3 + H_2 \ . \tag{4b}$$

Peroxy defects also exist in the structures of rock-forming minerals, feldspars and even olivine, $O_3X\text{-}OO\text{-}YO_3$ with X, Y = Si^{4+}, Al^{3+}, *etc*. Equation (5) describes schematically this solid state reaction sequence as given by Eqs. (4a, b).

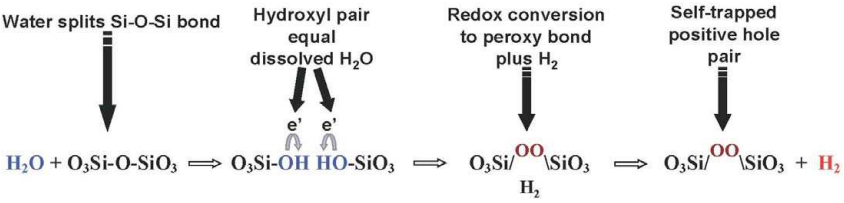

(5)

2.2 How peroxy defects break and release positive hole charge carriers

It now appears certain that peroxy defects are ubiquitous in the mineral world. Every igneous rock in the Earth's crust that crystallized from an H_2O–laden magma and every high-grade metamorphic rock that recrystallized in a high-temperature H_2O–rich environment takes up a finite amount of H_2O component in the form of hydroxyls, $O_3Si\text{-}OH$. Upon cooling the majority of these hydroxyls undergo the redox conversion, by which the rocks acquire a non-zero complement of peroxy defects. Peroxy defects will also be present in any sedimentary rock that contains detrital mineral grains from igneous and high-grade metamorphic rocks such as sandstones, limestones, arcoses, *etc*.

The presence of peroxy defects in the matrix of rock-forming minerals has far-reaching consequences with respect to the capability of the rocks to: (i) generate electronic charge carriers when subjected to tectonic stresses, and (ii) allow those electronic charge carriers to flow and carry a current.

The structure of every silicate mineral is made up of large O^{2-} anions filling most of the space and the usually much smaller metal cations. The O^{2-}–O^{2-} distance is typically around 2.8-3.0 Å. Two O^- bonded together form a peroxy link with a very short O^-–O^- distance around 1.5 Å. The volume occupied by two O^- in the peroxy bond is almost the same at the volume of a single O^{2-}. For this reason peroxy defects in minerals are inconspicuous and their presence has escaped the attention of the geoscience community for a long time.

Peroxy defects are electrically inactive. They break up, however, when stresses are applied (Freund *et al*. 2006). Low to moderate stress levels will cause mineral grains to slide past each other, high stress levels can cause plastic deformation due to the action of dislocations, which move through the mineral grains causing zipper-like displacements of rows of atoms in the structure. Each time a peroxy link is perturbed, the O^-–O^- bond is likely to break. A neighboring O^{2-} then acts as an electron donor sending an electron into the broken peroxy bond as outlined in Eq. (6):

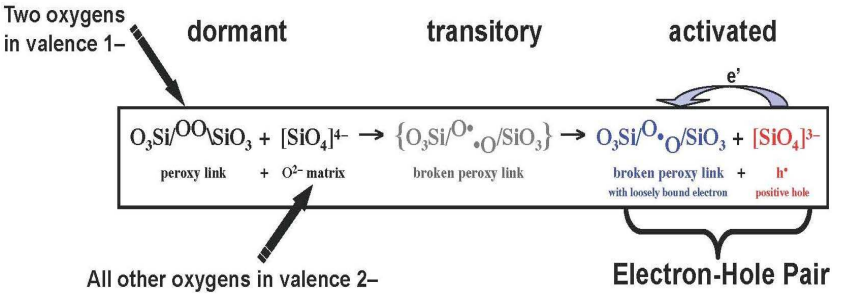

(6)

The broken peroxy bond acts as electron receptor, while the O^{2-} in the $[SiO_4]^{4-}$, which donated the electron, turns into O^-, *i.e*., a positive hole symbolized by $h^\bullet$.

The $h^\bullet$ travel through mineral grains and can cross grain boundaries. They can propagate from grain to grain in compact rocks and from grain to grain in sand or soil as long as the mineral grains maintain physical contact.

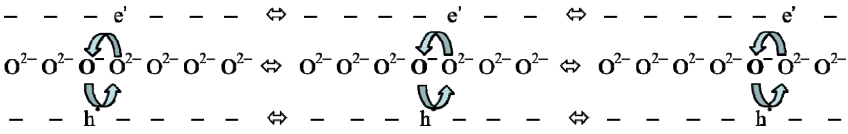

(7)

When positive holes propagate in one direction, electrons hop from O^{2-} to O^- in the opposite direction as indicated by Eq. (7). In essence, each time two oxygens vibrate against each other and the O–O distance gets shorter, the overlap of their electronic wave functions increases exponentially, enabling an electron to hop. The vibrations occur at the frequency of thermal phonons, about 10^{12} Hz. With each hop the $h^\bullet$ advance by ~2.8 Å. Thus the maximum speed with which an $h^\bullet$ pulse can propagate will be $2.8 \cdot 10^{-10} \times 10^{12}$ equal to 280 m s^{-1}. The measured phase velocities of $h^\bullet$ through various rocks are 200-300 m s^{-1} (Freund 2002, Hollerman *et al*. 2006), consistent with such a phonon-assisted electron hopping mechanism (Shluger *et al*.

1992). The activation energy, *e.g.*, the height of the energy barrier over which the electrons have to hop in order for the $h^{\bullet}$ to move, is on the order of 1 eV. The drift velocity of an actual $h^{\bullet}$ wave spreading along its self-generated electric field gradient will be significantly lower.

During the lead-up to any earthquake, tectonic forces will subject rocks to increasing stresses. Deformation will happen on all scales, from grain-grain slippage to microscopic contact points between grains that act as stress concentrators, to large bulk volumes comprising hundreds to thousands of km^3 of rocks, sometimes possibly tens to hundreds of thousand of km^3. However, long before the stresses reach values high enough to cause catastrophic rupture, the dormant peroxy defects will "wake up", activating $h^{\bullet}$ charge carriers. The numbers of $h^{\bullet}$ will scale with the volume of the rocks that is being stressed and with the rate at which the stresses are applied. An important question therefore arises: if precursory signals start to be generated when the total number of $h^{\bullet}$ charge carriers activated reaches or exceeds certain (as yet unknown) threshold values, we would expect a correlation between the intensity and areal extent of these precursory signals and the magnitude of the earthquake, which is to follow.

3. CONSEQUENCES OF STRESS-ACTIVATION OF POSITIVE HOLES

3.1 Flow of positive hole charge carriers through the bulk

Uniaxial loading of one end of a rock can simulate the build-up of tectonic stresses before major seismic events. The stresses activate $h^{\bullet}$ charge carriers alongside electrons e'. The $h^{\bullet}$ are mobile and capable of spreading out of the stressed rock into the adjacent unstressed rock volume, while the e' remain trapped at the sites of the broken peroxy bonds as indicated by Eq. (6) (Freund 2002, Freund *et al*. 2006). The application of stress causes the concentrations of $h^{\bullet}$ and e' to increase inside the stressed subvolume as outlined on the left side at the bottom of Fig. 1.

The situation described by Fig. 1 is similar to that in a battery. The difference is that, in the case of an electrochemical battery, the charges flowing out of the anode into the electrolyte are metal cations. The electrons cannot flow through the electrolyte. In order to close the battery circuit a metal wire is needed. A "rock battery" differs from an electrochemical battery in as much as the positive charges flowing out of a stressed rock are electronic in nature, positive holes, $h^{\bullet}$. Thus a stressed rock in contact with an unstressed rock is a semiconductor battery that is driven by the concentration gradient of $h^{\bullet}$ charge carriers along the stress gradient.

However, a sustained current outflow can take place only if and when the battery circuit is closed. Circuit closure is easily achieved in laboratory

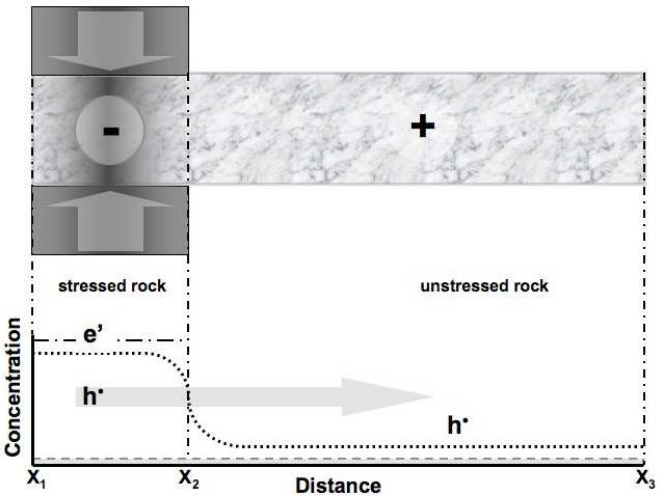

Fig. 1. Schematic representation of the activation of positive holes, which flow out of the stressed rock volume. Bottom: Before application of stress the $h^{\bullet}$ concentration is low and uniform throughout the rock (dashed line). After application of stress the concentration of e′ and $h^{\bullet}$ increases in the stressed subvolume (dot-dashed). The $h^{\bullet}$ out-flow causes the $h^{\bullet}$ concentration in the stressed rock decrease and in the unstressed rock to increase (dotted). The unstressed rock becomes positively charged relative to the stressed rock.

experiments by placing a Cu electrode on the unstressed end of the rock and running a wire to the pistons, which are in electrical contact with the stressed portion of the rock as sketched in Fig. 2a. Circuit closure in the Earth's crust is of course not that easy.

One of several possible routes toward circuit closure can be provided by an electrochemically conductive path. Using a set-up as depicted in Fig. 2b it has been shown that, when $h^{\bullet}$ charge carriers arrive at a rock-water interface, they oxidize H_2O stoichiometrically to H_2O_2 (Balk *et al*. 2009). The current continues to flow through the water in form of an electrolytical current, probably carried by H_3O^+. Recognizing this feature has allowed us to build a "rock battery" as depicted in Fig. 2c, in which circuit closure was provided through a water-filled capillary connecting a water bath at the unstressed end of the rock with a water bath attached to the stressed portion of the rock. In the absence of a Cu wire and an ammeter, closure of the circuit was ascertained by monitoring the on-set of H_2O_2 formation in the water bath at the unstressed end (Balk *et al*. 2009).

A possible case where such electrolytical circuit closure seems to have been achieved in the field prior to a large earthquake in Taiwan has been discussed elsewhere (Freund and Pilorz 2012).

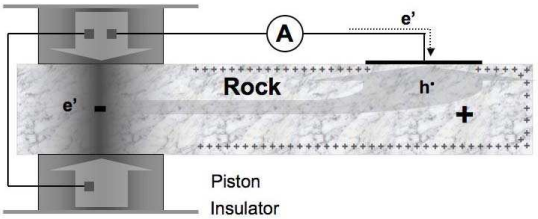

Fig. 2a. Set-up to measure the battery current with a Cu contact placed on the rock.

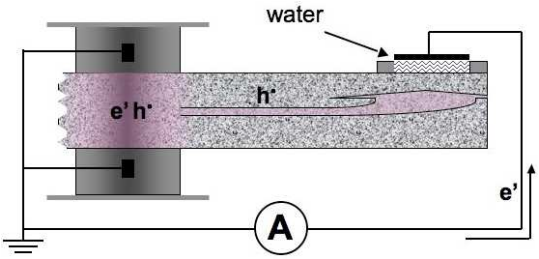

Fig. 2b. Set-up to measure the current by letting it flow through water.

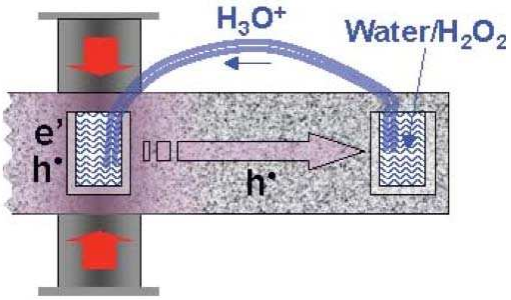

Fig. 2c. Set-up to close the battery circuit by means of an electrolytically conductive pathway.

3.2 Air ionization at the ground-to-air interface

When mobile charge carriers of the same sign, either positive or negative, are injected into a dielectric medium, they repel each other in the bulk. They form a subsurface charge layer, which creates a constant surface potential to be measured in volts, V (King and Freund 1984). The activation of positive hole charge carriers in a rock creates such a situation. The higher the number density of the charges in the bulk, the thinner the subsurface charge layer.

We now turn to the electric field E, which is defined as V/d, where d is the distance. Though the surface potential stays constant, the E field in the surface/subsurface layer increases rapidly with increasing number density of the mobile charge carriers in the bulk and, hence, with decreasing thickness of the charge layer. If there is a short-range E field beneath the surface, there is also a short-range E field of similar values above the surface. The relevant dimensions are in nanometers, 1 nm = 10^{-9} m. While the surface/subsurface

E field of interest here is felt only in the immediate vicinity of the surface itself, this is enough to affect any air molecules, which touch the surface: they will be exposed to a very steep *E* field.

Three processes can be recognized that will take at the ground-to-air interface when positive hole charge carriers, stress-activated deep below, arrive at the Earth surface.

Step I: As positive hole charge carriers, stress-activated deep below, arrive at the Earth surface, an increasingly steep positive *E* field builds up at the surface.

Step II: If the surface potential reaches ~2 V, the *E* field will reach values on the order of 10^6 V/cm or more, high enough to field-ionize air molecules. The most likely first candidate for field-ionization is O_2 because it has a relatively low ionization threshold.

Step III: If the *E* field at the surface increases even further, it can reach values sufficient to accelerate free electrons, which are always available in air in small numbers due to cosmic rays and the omnipresence of radon. If these electrons are accelerated to kinetic energies sufficiently high to impact-ionize neutral air molecules and generate more free electrons, ionization avalanches will take place leading to corona discharges. These corona discharges will occur preferentially at points, edges and corners, where the subsurface charge accumulation is highest.

To study the possibility of field-ionization of air due to the accumulation of positive holes in the subsurface a laboratory set-up was used as depicted in Fig. 3a, where a metal plate above the rock surface acts as a non-contact capacitive sensor. It was shown that, as soon as one end of the rock was loaded, the other end developed a pronounced positive surface potential. The positive surface potential rose rapidly to 2-3 V and then abruptly changed to negative values. By biasing the capacitive sensor either negatively or positively, the capacitive sensor can be turned into an ion collector to monitor positively ionized air molecules or negatively ionized air molecules and free electrons generated on the rock surface, respectively (Freund *et al*. 2009).

The implementation of these laboratory experiments has led to the demonstration of the sequence of events consistent with Stage I-III (Freund *et al*. 2009).

Specifically, with respect to Stage I, we observed upon first application of stress a rapid build-up of a pronounced positive surface potential reaching 2-3 V, strong oscillations, followed by a sudden change to a weakly negative surface potential. The fluctuations continued into the region of the negative surface potential and even became faster. With respect to Stage II and III, we recorded pulses of positive airborne ions generated at the rock surface during the positive surface potential fluctuations. The abrupt change of the surface to negative values was accompanied by a sudden on-set of corona discharges,

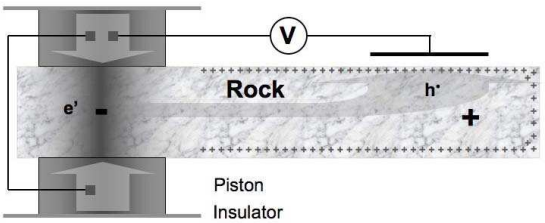

Fig. 3a. Set-up to measure Step I: surface potential with a non-contact capacitive sensor.

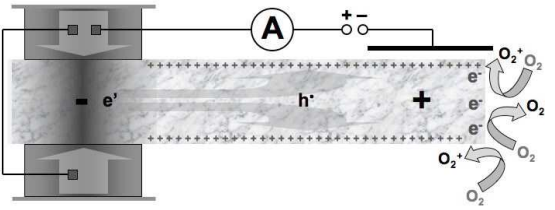

Fig. 3b. Set-up to measure Step II: air ionization with a negatively bias ion collector and formation of positive airborne ions.

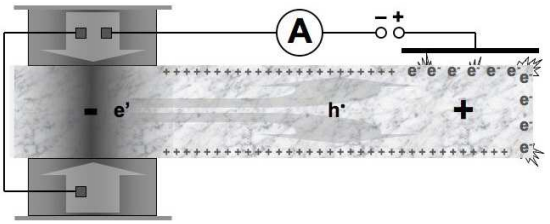

Fig. 3c. Set-up to measure Step III: air ionization with a positively bias ion collector and formation of free electrons and negatively charged air ions during corona discharges.

leading to bursts of both electrons and negative airborne ions, plus positive airborne ions. The rates at which the airborne ions were produced at the flat rock surface with some edges and corners appear to be on the order of 10^7-10^9 s^{-1} cm^{-2}. Figure 4 summarizes these laboratory observations.

These laboratory experiments do seem to be directly relevant to field observations. There is strong evidence that, prior to major earthquakes, the air above the epicentral regions becomes ionized, sometimes forming exclusively positive ions, sometimes a mixture of positive and negative ions (Bleier *et al*. 2010, 2012, e-PISCO 2012). The air ionization seems to take place in pulses, at times merging into intense ionization episodes lasting for many hours.

Figure 5 shows an example of regional air ionization measured at the PISCO station in Kanagawa, southwest of Tokyo. The plots cover two overlapping periods in June/July 2008. Positive air ion concentrations are plotted upward, negative air ion concentrations downward. The "Attention Line" is drawn at 50 *x* the fair-weather value of ~200 ions cm^{-3}. There are several periods of exclusively or predominantly positive airborne ions, in particular on 15 June and 02/03 July 2008, the latter followed by a long period of high

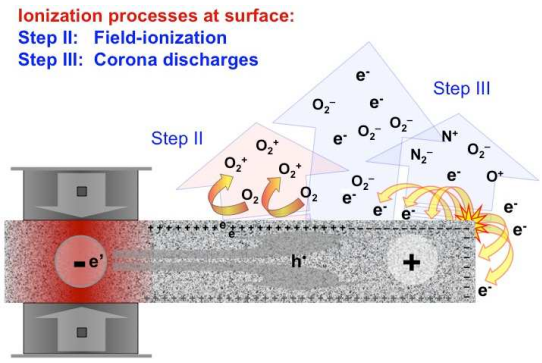

Fig. 4. Schematic representation of: (i) the production of massive amounts positive airborne ions during Stage II, when the potential at the rock surface was positive, and (ii) the on-set of corona discharges during Stage III, producing bursts of free electrons as well as of positive and negative airborne ions, when the potential at the rock surface turned negative.

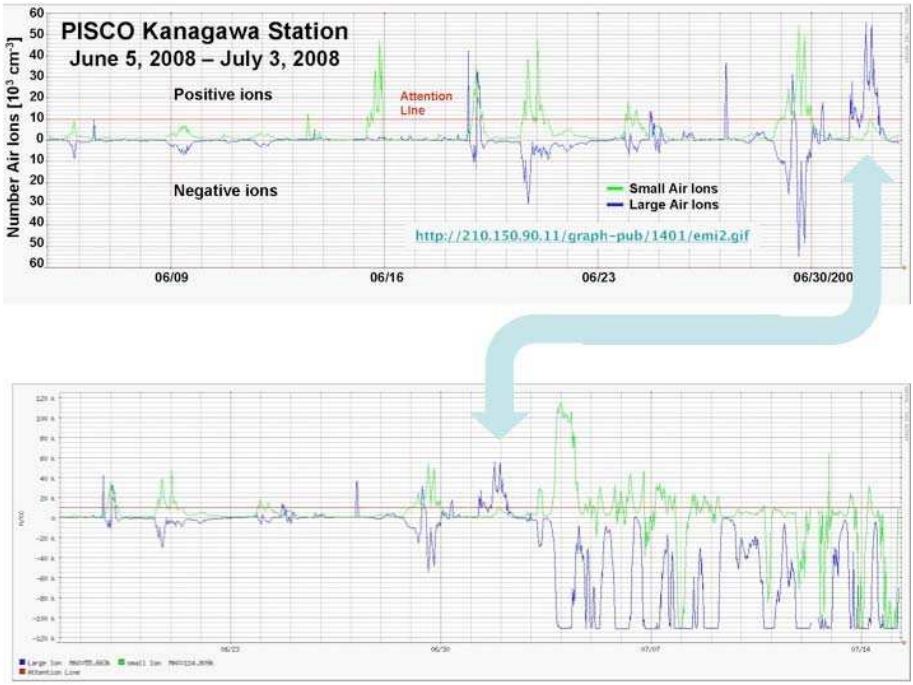

Fig. 5. Regional air ionization measured at the PISCO station in Kanagawa, Japan, covering two overlapping 4 week periods in June/July 2008. Positive and negative air ion concentrations are plotted upward and downward, respectively. Green – small airborne ions, blue – large ions and aerosols. Colour version of this figure is available in electronic edition only.

concentrations of predominantly negative ions, presumably aerosols, prevalent during night-time (e-PISCO 2012).

Of special interest in the context of pre-earthquake phenomena are periods, when exclusively or predominantly positive airborne ions are generated at the ground-to-air interface. This situation is expected to occur when positive hole charge carriers, stress-activated deep below, first arrive in sufficiently large numbers at the Earth surface begin to field-ionize air molecules. According to the laboratory experiments mentioned the rate at which exclusively positive airborne ions are generated may be as high as 10^7 s^{-1} cm^{-2} (Freund *et al*. 2009). If such a massive air ionization takes place over a relatively wide region, say > 100 km across, it will certainly have far-reaching consequences across the entire atmospheric column and well into the ionosphere (Rycroft *et al*. 2008, Sapkota and Varshneya 1990, Singh *et al*. 2011).

3.3 Potential difference between Earth's surface and ionosphere

To consider the predictable consequences of air ionization at the ground-to-air interface we have to consider the electric field between the Earth surface and the lower edge of the ionosphere.

A large potential difference is believed to exist between the Earth surface and the ionosphere, on the order of 150 to 500 kV with 250 kV quoted as a typical value (Rycroft *et al.* 2000, 2008, Sapkota and Varshneya 1990, Singh *et al.* 2011). Under fair weather conditions a positive current, globally about 1 kA, flows from the ionosphere downward to the Earth surface as indicated in Fig. 6a (Golkowski *et al*. 2009) indicating that the ionosphere is positive relative to the ground and, hence, that the ground is negative. Such a negative Earth surface would act either as a sink for positive charges arriving from above or as a source for electrons flowing upward or a combination of both.

Schematic drawings of the global electric circuit invariably include thunderstorm clouds where the tops are marked positive and the undersides negative as depicted in Fig. 6a (Kubicki 2011). A positive current flows upward from the top of the thundercloud to the ionosphere, carried by positive ions, while the negative charge, which accumulates at the bottom of the cloud, attracts positive charges in the ground. Downward lightning strikes would then deliver electrons to the ground in response to the positive charges that have accumulated there. The conclusion to be drawn from this dichotomy is that, under thunderstorm conditions, the polarity of the global electric field should be opposite to that prevailing under fair weather conditions.

We can look at the thundercloud as a system, in which internal convections transport positively charged small water droplets or ice crystals up-

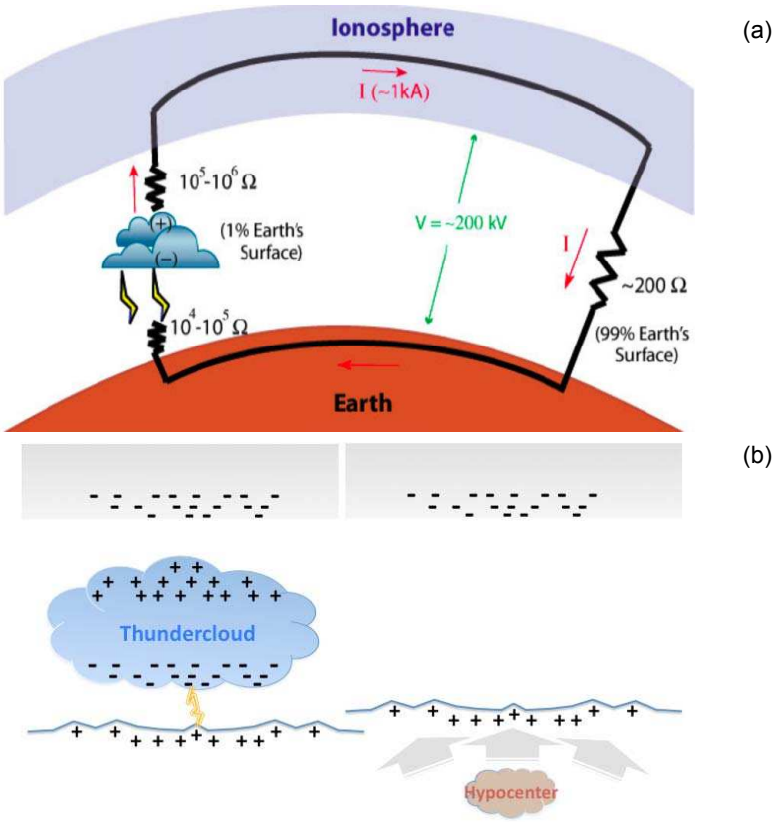

Fig. 6: (a) Schematic drawings of the Earth's Global Electrical Circuit (Kubicki 2011), (b) two-plate capacitor with a cloud as a polarizable medium and under pre-earthquake conditions.

ward, leaving behind negatively charged larger water droplets or ice crystals in the lower part of the thundercloud as depicted in Fig. 3b (left). In the context of the global electric circuit this charge separation within the thundercloud is believed to be the "engine" that drives an accumulation of negative charges at the lower edge of the ionosphere and an accumulation of positive charges on the surface of the Earth (Rycroft *et al.* 2000).

Taking the Earth–ionosphere system as a 2-plate capacitor this scenario is depicted on the left side of Fig. 6b, where the charge separation in the thundercloud, due to active convection, is the primary process which induces a negative charge in the ionosphere and a positive charge in the ground. Taking the fair weather condition as "normal", thunderclouds would therefore create an anomaly, namely a reversal of the polarity both in the ionosphere and in the ground.

On the right side of Fig. 6b a similar scenario is sketched, one to be derived from the observation that, prior to major earthquakes, the Earth surface becomes positively charged, even in the absence of a thunderstorm overhead. In this case the stress activation of positive hole charge carriers in the Earth crust and their arrival at the surface are the driver of the positive charge onn the ground. In this scenario, the positive surface charge is not induced by a thundercloud but driven from within the Earth crust. If the ground is positive, the ionosphere must be negative.

Papers, which contain depictions as exemplified in Fig. 6a, often state that the Earth's ground is negative and that, relative to the ground, the lower edge of the ionosphere is positive. Gish and Wait (1950) write: "the direction of the current, in the conventional sense, is upward in all cases, thus indicating that the net charge transported from thunderstorms to earth is negative", followed by the statement: "This result supports the view that thunderstorms do maintain the general negative charge of the earth." Similar statements are found in recent papers (Rycroft *et al*. 2000, 2007, 2008, Harrison *et al.* 2010)

The idea of a negatively charged Earth surface appears to come from the observation that the air near ground level tends to be more highly ionized than the air higher up and that it contains more positive ions than negative ions (Harrison and Bennett 2007, Hoppel *et al.* 1986, Rycroft *et al.* 2008). One possible interpretation is that the ground is negative and therefore attracts positive ions. However, on the basis of the work presented here it can be said with confidence that positive holes are the dominant mobile charge carriers in the Earth's crust and that they accumulate at the Earth surface. If their number density becomes high, the positive holes can cause field-ionization of air molecules, thereby selectively producing positive airborne ions (Freund *et al.* 2009). This provides an alternative interpretation for an excess of positive airborne ions near the Earth surface: the excess is not caused by selective attraction of positive airborne ions to a presumably negative ground but by the Earth ground acting as a source of positive airborne ions.

3.4 Ionized air bubble rising

When air molecules are ionized, for instance by solar UV radiation, cosmic rays or radon decay, they form electrons and positive ions. Electrons and positive ions have a tendency to recombine near-instantly. Electrons also attach themselves to neutral gas molecules forming negative molecular ions. Positive and negative air ions attract each other and will have the tendency to neutralize. By contrast, if only positive airborne ions are generated by the field-ionization at ground level, we arrive at a very different situation: posi-

tive airborne ions cannot neutralize. Hence, an air volume laden with positive airborne ions will be stable for a long time.

If pre-earthquake field-ionization takes place over relatively wide areas, on the order of 100 km across, the positively charged air bubble will expand due to its internal electrostatic repulsion. The only direction it can expand is upward, possibly up to stratosphere heights. In addition, within the framework of a negatively charged lower edge of the ionosphere, relative to the Earth ground, we can expect that the prevailing *E* field will accelerate positive airborne ions upward.

On the way up, if the relative humidity at any height is in the right range, the airborne ions will act as condensation nuclei for water droplets to form. Hence cloud formation should be expected to occur preferentially over areas, where massive positive air ionization takes place at the ground level, subject to prevailing winds (Guo and Wang 2008). During condensation latent heat will be released, raising the temperature of the air, causing additional updrift and anomalous increase in the intensity of the outgoing infrared radiation, especially in the long wavelength region, which is being monitored as part of worldwide efforts to derive pre-earthquake information from thermal infrared (TIR) anomalies seen in satellite infrared images (Kafatos *et al.* 2010, Qin and Wu 2012, Saraf *et al*. 2012, Tramutoli *et al.* 2005).

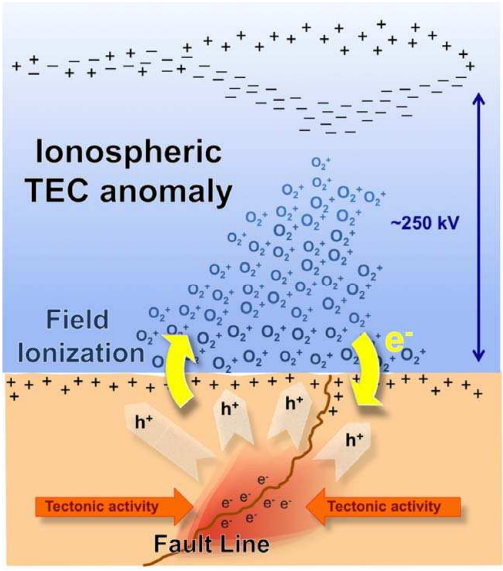

Fig. 7. Air bubble, laden with positive airborne ions generated at the ground-to-air interface, expanding upward through the atmosphere column, dragging along the Earth's ground potential, and eliciting a polarization response in the ionosphere, which leads to a redistribution of the electrons at its lower edge.

Because of the increased electrical conductivity of an upward expanding ion-laden air volume, such an air bubble will drag along part of Earth's ground potential. It will shorten the distance over which the vertical potential difference decays between the Earth's ground and the ionosphere. In response the ionospheric plasma is expected to polarize, causing electrons at its lower edge to be pulled downward as schematically depicted in Fig. 7.

Thus an induced polarization of the ionospheric plasma would provide the basic mechanism for the widely reported increase in the Total Electron Content (TEC) in the lower part of the ionosphere before major earthquakes. TEC is defined as the total electron content along the path of the GPS beacon, relative to an average value. The units are given in number of electrons per square meter along the path (Liu *et al*. 2004, 2010, Ondoh 2003, Pulinets *et al*. 2005). More recently data from multiple ground stations and multiple satellite-based GPS beacons are being used to reconstruct a tomographic

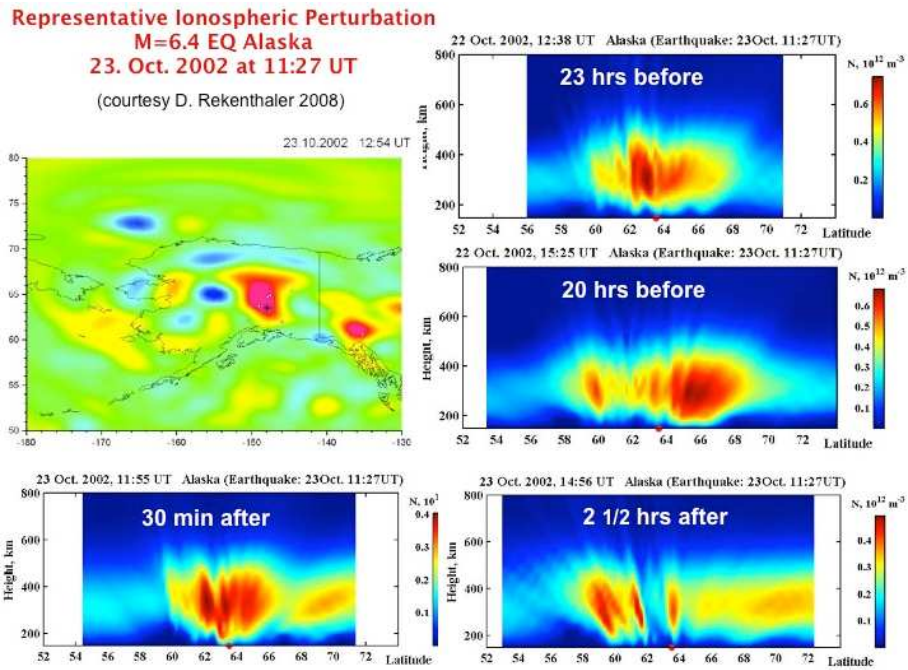

Fig. 8. Upper left: 2-dimensional projection of the TEC anomaly on the map of Alaska with the epicenter of the *M*6.4 earthquake of 23 October 2002 marked by +. Local time of the event was 02:27 a.m. Left side and below: TEC concentrations in units of 10^{12} electrons m^{-3} at different times before and after the earthquake as a function of height in a N-S plane through the epicenter. The vertical direction toward the epicenter is marked by a red dot. Colour version of this figure is available only in electronic version.

image of the electron density in the ionosphere. Here the number of electrons the number of electrons per unit volume is given in units of 10^{12} m^{-3}, often referred to as TECU. An example is shown in Fig. 8 for the TEC anomaly prior to a *M*6.4 earthquake in Alaska on 23 October 2002. In the upper left side panel the anomaly is projected onto the map of Alaska. The other panels show four vertical sections in the N-S plane through the epicenter shortly before and after the earthquake.

Within the framework of the simple 2-plate capacitor considered here, the electrons in the ionosphere are pulled downward in response to positive airborne ions rising upward from the ground. In laboratory experiments, the rate at which positive ions were generated at the surface of a block of rock submitted to stress at one end had been found to be on the order of 10^7 cm^{-2} s^{-1} (Freund *et al.* 2009). Assuming that positive airborne ions would be generated at the surface of the Earth at a similar rate, prior to a major earthquake, it could conceivably explain the total number of electrons causing the TEC anomaly.

3.5 Role of radon

The analysis presented here reveals a weakness of the widely publicized idea that radon emanation from the ground, possibly due to microfracturing, would be responsible for the increase in air ionization at the ground level and for essentially all salient features of the pre-EQ LAI coupling model (Dunajecka and Pulinets 2005, Kamsali *et al.* 2011, Omori *et al.* 2009, Pulinets 2007, Pulinets and Ouzounov 2011). The average number of Rn atoms in air at sea level is 150 cm^{-3} (Linde-Gas 1995), of which 1/2 will decay within the half life of ^{222}Rn, 3.8 days, equivalent to about 300 000 s. This gives a steady-state decay rate per liter air (1000 cm^3) of less than 0.25 s^{-1} or 1 decay event per cm^3 every 4000 s.

Figure 9 shows the contributions to the ionization rates in near-surface air due to backscattered beta and gamma rays from the decay of radioactive elements in the Earth, cosmic rays and radon (Gringel *et al.* 1986). The contribution from beta and gamma rays amounts to about 20 ions cm^{-3} s^{-1} at the surface, decreasing to nil within the first 100-200 m. The contribution from cosmic rays is about 2 ions cm^{-3} s^{-1} and constant below 1000 m. The contribution from radon varies regionally, from about 30-300 ions cm^{-3} s^{-1} at the Earth's surface, typically decreasing to less than 5 ions cm^{-3} s^{-1} at 1000 m above the surface.

As an alpha emitter with an energy of about 5.8 MeV per decay event, each ^{222}Rn atom generates about 10^5 electron-ion pairs in the air (Nagaraja *et al.* 2003). Many of the electron-ion pairs can be expected to recombine near-instantly, consistent with the reported low ionization rate of 30-300

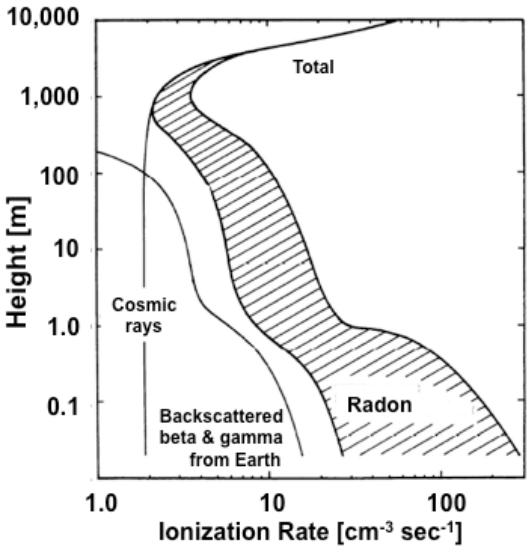

Fig. 9. Average rate of air ionization in the first 10 km of the atmosphere under "fair weather" conditions due to radon, cosmic rays, and back-scattered beta and gamma radiation from the ground (after Gringel *et al.* 1986, Hoppel *et al*. 1986).

ions cm^{-3} $s^{-}1$ that can be attributed to ^{222}Rn (Gringel *et al.* 1986, Hoppel *et al.* 1986). Changes in the radon emanation rate that appear to be linked to tectonic activity do occur, but they are usually on the order of a factor of 2-4, rarely up to 10 (İnan *et al.* 2008, 2010, Moura *et al.* 2011, Nagaraja *et al.* 2003).

By contrast, the production rates of airborne ions due to field-ionization of air molecules and/or to corona discharges at the Earth surface appear to be orders of magnitudes higher, possibly as high as 10^7-10^9 s^{-1} cm^{-2} as determined in laboratory experiments (Freund *et al.* 2009) and consistent with data from the PISCO network in Japan (e-PISCO 2012). Those airborne ions, formed by field-ionization at the ground-to-air interface upon arrival of positive hole charge carriers from below, are more likely to be responsible for the diversity of atmospheric-mesospheric-ionospheric phenomena reported in the context of pre-EQ activity.

3.6 Mesospheric lightning and ripples in the ionospheric *E* field

If and when the upward expanding air bubble, laden with positive airborne ions, reaches the top of the stratosphere, positive ions will continue to experience the prevailing *E* field, which pulls them further up toward the lower edge of the ionosphere. As the gas pressure decreases with increasing height, the mean free path between collisions of the ions with gas neutrals increases. As a consequence, the upward movement of positive ions through the mesosphere is expected to transition from a slow upward drift to an ever faster upward flow.

Within the boundary conditions put forth here we postulate that the upward flow of positive ions through the mesosphere will initially be homogeneous, covering a large cross section, on the order of tens to possibly hundreds of kilometers for large earthquakes. In the ever improving vacuum the ions will move faster and faster upward. If the number density of ions per unit volume reaches or exceeds some critical value, the magnetic field generated by the upward ion flow will couple to the Earth's dipole field, causing magneto-hydrodynamic instabilities to develop in the current field. As a result, as depicted in the central part of Fig. 10, the homogeneous current will break up into patches of higher and lower ion concentrations. As a result, potential differences will develop within the mesosphere. This in turn will lead to *E* fields between different patches. It is still unknown whether the *E* fields can reach values sufficiently high to trigger mesospheric lightning discharges as indicated in Fig. 10. However, the possibility of such lightning above

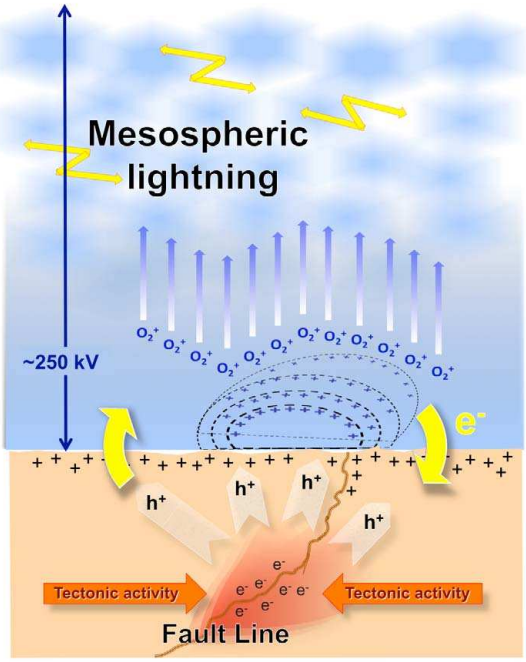

Fig. 10. Expected processes in the mesosphere above the epicentral area of an impending major earthquake: if massive air ionization takes place at the Earth surface over a large area around a future epicenter, generating positive airborne ions, the air laden with positive ions will expand upward, possibly to the top of the stratosphere. From there the ions will continue to be accelerated upward. However, the ion current is expected to break up into regions of higher and lower ion densities. This could cause mesospheric lightning and ripples in the *E* field in the ionosphere.

the epicentral areas of impending large earthquakes will certainly have to be considered (Kuo 2012).

The break-up of an initially homogeneous upward ion current into patches of different ion densities in the mesosphere can be expected to lead to ripples in the *E* field in the ionosphere. These ripples will extend further up and may become detectable as turbulences when satellites cross over epicentral regions of impending large earthquakes. Based on data from the DEMETER mission such turbulences in the ionospheric *E* field have been reported (Blecki *et al.* 2011, 2010, Walker *et al.* 2012), lending support to the overall concept presented here.

Another predictable consequence of a vertical flow of positive ions through the mesosphere would be that, as the positively charged ion bubbles accelerate upward, the electrons at the lower edge of the ionosphere will respond by moving downward with the same speed. As the positive ion bubbles merge into the ionosphere, the electrons will relax and move up again. Modeling the speed of the upward positive ions flow, assuming a 250 kV potential difference between the Earth's ground and the ionosphere, gives values on the order of 10-30 m s^{-1} (Roberts and Freund 2012). These values are consistent with the recent report of ± 1-2 mHz Doppler shifts in the frequency of 60 kHz radio signals transmitted across areas where major earthquakes occurred (Hayakawa *et al.* 2012). Such Doppler shifts imply a dynamic vertical up and down movement of the ionospheric reflection layer with speeds on the order of ± 10-30 m s^{-1}.

In another context, in the context of sprites and other flashes above major thunderstorms, mesospheric lightning events have been extensively discussed in recent years. Sprites are very fast, low luminosity vertical electric discharges that have been anecdotally reported for a hundred years, often called "upward lightning". For decades, however, their existence has been called into question by the mainstream atmospheric community. Eventually, during a routine test of low-light video equipment intended to record a small rocket launch in 1989, mesospheric lightning was serendipitously documented for the first time. Soon thereafter sprites and related mesospheric discharges were accepted by mainstream science as a diverse and widespread phenomenon above large thunderstorm systems (Boeck *et al.* 1998, Pasko 2006).

In thunderstorms the vertical distribution of electric charges is such that the top of the clouds generally becomes positive, while the underside acquires a negative charge (Kuo 2012, Rycroft *et al.* 2007). Such a situation is not unlike the scenario postulated here for pre-EQ conditions, when positive airborne ions generated at the Earth surface would rise to stratospheric height and become available for further upward acceleration through the mesosphere. In both cases the flow of positive airborne ions can be expected

to have similar consequences higher up in the mesosphere and in the ionosphere directly above it.

4. DISCUSSION

Only a portion of the known or suspected pre-EQ phenomena has been mentioned in this report, essentially those phenomena that can be linked to ionization of air at the ground-to-air interface. Ground-level ionization events strong enough to be recorded on the Earth surface and to solicit an ionospheric TEC response appear to take place prior to many, if not all major earthquakes. There is strong evidence that, under certain conditions, exclusively positive airborne ions are generated. Their upward flow through the atmospheric into the mesosphere and further up to the ionosphere is the main topic presented here.

Vertical electric currents over the faults have been considered before in efforts to model ionospheric effects (Kuo *et al.* 2011, Namgaladze *et al.* 2012, Sorokin *et al.* 2005). Air ionization at the ground level has been documented in laboratory experiments (Freund *et al.* 2009) and confirmed by field observations (Bleier *et al.* 2010, e-PISCO 2012). The reasons for air ionization are rather well understood (King and Freund 1984), though open questions remain, which still need to be studied in greater detail.

Thermal infrared anomalies: For about 20 years there have been numerous reports of so-called thermal infrared (TIR) anomalies observed by satellite remote sensing to occur around or near the epicenters of impending major earthquakes several days before the events (Filizzola *et al.* 2004, Ouzounov *et al.* 2006, Saraf *et al.* 2008, Tramutoli *et al.* 2005, Tronin 1996). While most TIR anomalies reportedly occur over land, some seem to have observed over water for large, subduction-related earthquakes (Ouzounov *et al.* 2007, 2011). No widespread agreement exists as to the underlying physical cause or causes. Increased air ionization due to radon emanation from the ground has been quoted as a possibility or the release of trace gases causing a "local greenhouse effect" but the details remain unclear. A very different proposal is based on the recognition that, if positive holes arrive in large numbers at the Earth surface, they must have a finite probability to recombine to form again peroxy defects. We know that this process is exothermal, releasing slightly more than 2 eV per recombination event. Therefore, if two adjacent surface O^{2-} trap positive holes and recombine to form an O^{-}–O^{-} bond, they will have to absorb about 2 eV energy. They will become vibrationally excited. Since 2 eV is equivalent to a temperature of about 25 000 K, the most likely process by which these vibrationally highly excited oxygens can get rid of this much excess energy is by emitting infrared photons while tumbling down the quantum scale of their vibrational manifold.

The emission of such spectroscopically distinct IR photons has been experimentally confirmed (Freund *et al.* 2007) and may be the route cause of the reported pre-EQ TIR anomalies.

Physiological effects: Positive airborne ions have been known for many years to have remarkable physiological effects on humans and animals by increasing the level of the stress hormone serotonin in the blood (Hedge and Eleftherakis 1982, Krueger *et al.* 1968, Krueger and Reed 1976). Therefore, the generation of massive amounts of positive airborne ions might play a significant role in the response of humans and animals to pre-EQ conditions (Morton 1988, Shitov 2010).

In laboratory experiments, when stress on the rock samples is further increased, the generation of positive airborne ions is followed by the generation of positive plus negative ions, alongside rapid-fire light pulses. These observations are indicative of corona discharges that are triggered at the rock surface and produce even higher concentrations of airborne ions (Freund *et al.* 2009). According to field observations, the same firing of corona discharges appears to be taking place at the ground-to-air interface as a result of even larger stress build-up deep below.

Ionospheric effects: There are certainly consequences arising from the generation of both positive and negative airborne ions, different from the field-ionization production of positive ions alone. These consequences will include a different response of the atmospheric column and an expected increase in the broad-band radio-frequency noise due to the corona discharges (Biagi *et al.* 2001, Harrison *et al.* 2010), possibly even some faint luminous effects (Derr *et al.* 2011).

Obviously, since the medium is the ionosphere, many properties of the ionosphere will be affected, foremost the height at which radiowaves are reflected. A large body of literature exists related to these and other anomalous phenomena that have been identified (Hayakawa *et al.* 2010, Jhuang *et al.* 2010, Liu *et al.* 2010, 2011, Namgaladze *et al.* 2012).

Electrochemical effects: Another group of suspected or confirmed pre-EQ phenomena appears to be produced by the electrochemistry taking place at the ground-water interface, when stress-activated positive hole charge carriers flow into water. It has been shown that, when the $h^{\bullet}$ charge carriers arrive at a rock-water interface, they change from being an electronic charge carrier to being a highly oxidizing O^{-} radical, •O, capable of "ripping off" an H atom from an H_2O and turning it into an •OH radical. Two •OH radicals combine to form an H_2O_2 molecule (Balk *et al.* 2009).

As a result of this reaction, the O^{-} at the rock-water interface turns into an OH^{-}, thereby causing the rock surface to turn into a hydrous gel – a process that can be viewed as a form of electro-corrosion of the rock. This electro-corrosion is predicted to lead to an accelerated release of cations from the

rock into the water. This process has been confirmed by laboratory experiments (Grant *et al.* 2011) and by measuring the changes in the cation concentrations in spring waters before and after the *M*7.2 Van earthquake in Eastern Turkey on 23 October 2011 (Inan *et al.* 2012). Electro-corrosion of rocks driven by the stress activation of positive hole charge carriers deep below appears to also be the reason behind some other reports of distinct pre-EQ changes in ground or spring water chemistry (Claesson *et al.* 2004, Pérez *et al.* 2008).

Currents in the Earth crust: Another ensemble of reported pre-EQ phenomena that has been left out of the discussion presented here derives from processes, which take place inside the Earth's crust, when positive hole charge carriers become stress-activated and begin to flow out of the stressed rock volume.

In the literature much has been said about microfracturing of rocks as a process that would lead to the electrification of the rocks in the Earth crust (Eftaxias *et al.* 2009, Molchanov and Hayakawa 1998, Liu and Liu 1997, Vallianatos and Triantis 2008, Yoshida and Ogawa 2004). Most of the studies on which these ideas are based have been done in the laboratory with unconfined or only partly confined rock cylinders subjected to increasing stresses up to failure. Under these conditions the cylinders deform to a pillow shape and tensile stresses build up, leading to the opening of fractures. A wide range of EM emissions can be observed from x-rays, visible light, infrared and microwave frequencies to low and ultralow frequencies. They are, in essence, due to charge separation on the atomic scale, when cracks form and opposite sides of cracks are pulled apart. It is questionable to what extent analogous fracturing and microfracturing events actually can take place deep inside the Earth crust, in and around the seismogenic zone, under the lithostatic overload of tens of kilometers of rocks. Since all EM waves except those with frequencies in the ultralow frequency (ULF) range, < 19 Hz, are quickly attenuated inside the crust, there is no chance to detect at the surface of the Earth any of the higher frequency emissions. By contrast, ULF waves have been documented, presumably emitted from deep below (Dea *et al.* 1997, Fraser-Smith 1992, Ohta *et al.* 2001). However, doubts as to the seismogenic nature of these ULF waves have also been voiced (Masci 2011, Thomas *et al.* 2009).

Obviously, when electric charges are mobilized in a rock under stress and flow out of this rock volume, they constitute a current. Any such current will generate a magnetic field. If the current fluctuates, EM radiation will be emitted at the frequencies, at which the current waxes and wanes. If the charge carriers are stress-activated positive holes that tend to flow down a stress gradient, a sustained current can only be obtained by closing the circuit as depicted in Fig. 2a.

While it is easy to achieve circuit closure in laboratory experiments as noted above, in nature, in the Earth crust, other conductive pathways have to be made available to allow for a current return path. One possibility, sketched in Fig. 2b, c, is to use the electrolytical conductivity of water or brine to close the circuit (Freund and Pilorz 2012). Other possibilities have been proposed such as the closure of the circuit through the electron-conductive (*n*-type) lower crust or through the air ions above the epicentral region (Freund and Pilorz 2012).

5. SUMMARY

It appears that the discovery of the positive hole, $h^{\bullet}$, their omnipresence in crustal rocks, albeit in a metastable state, and their particular properties as highly mobile electronic charge carriers has laid the basis for significant progress in understanding the wide range of pre-EQ phenomena that have been reported over the course of decades, even centuries and millennia. To continue and expand this work a broadly based multidisciplinary approach will be needed.

Acknowledgments. The work reported here has evolved over a period of more than 30 years. It has benefited from innumerable discussions with students and colleagues, whose names are listed in the referenced papers. In recent years I acknowledge many fruitful discussions and joint experiments with Dr. Akihiro Takeuchi, Dr. Bobby Lau, Dr. Robert Dahlgren, Dr. Stuart Pilorz, and bright-eyed students. Much of the basic solid state physics concept of positive hole charge carriers evolved through my collaboration with Dr. Minoru Freund, my son who died in early 2012, in the prime of his life, after a long, unwinnable battle with cancer. I thank Marek Golkowski for permission to use his schematics for Fig. 6a. My special thanks go to Morris Cohen, Georgia Institute of Technology, for advice on the Global Electric Cirucit. Funding for this work has come from NASA Goddard Space Flight Center through its GEST Scholarship Program, from the NASA Earth Surface and Interior program (Dr. John LaBrecque) and the NASA Exobiology Program (Dr. Michael New) as well as from the NASA Ames Research Center under the leadership of Dr. Pete Worden.

References

Balk, M., M. Bose, G. Ertem, D.A. Rogoff, L.J. Rothschild, and F.T. Freund (2009), Oxidation of water to hydrogen peroxide at the rock-water interface due to stress-activated electric currents in rocks, *Earth Planet. Sci. Lett*. **283**, 1-4, 87-92, DOI: 10.1016/j.epsl.2009.03.044.

Batllo, F., R.C. LeRoy, K. Parvin, F. Freund, and M.M. Freund (1991), Positive holes in magnesium oxide. Correlation between magnetic, electric, and dielectric anomalies, *J. Appl. Phys*. **69**, 8, 6031-6033, DOI: 10.1063/1.347807.

Biagi, P.F., R. Piccolo, A. Ermini, S. Martellucci, C. Bellecci, M. Hayakawa, V. Capozzi, and S.P. Kingsley (2001), Possible earthquake precursors revealed by LF radio signals, *Nat. Hazards Earth Syst. Sci*. **1**, 1/2, 99-104, DOI: 10.5194/nhess-1-99-2001.

Bleier, T., C. Dunson, C. Alvarez, F. Freund, and R. Dahlgren (2010), Correlation of pre-earthquake electromagnetic signals with laboratory and field rock experiments, *Nat. Hazards Earth Syst. Sci*. **10**, 9, 1965-1975, DOI: 10.5194/nhess-10-1965-2010.

Bleier, T., C. Dunson, S. Roth, J. Heroud, A. Lisa, F. Freund, R. Dahlgren, R. Bamberry, and N. Bryant (2012), Ground-based and space-based electromagnetic monitoring for pre-earthquake signals. **In:** M. Hayakawa (ed.), *The Frontier of Earthquake Prediction Studies*, Nihon-senmontosho-Shuppan, Tokyo, 282-305.

Błęcki, J., M. Parrot, and R. Wronowski (2010), Studies of the electromagnetic field variations in ELF frequency range registered by DEMETER over the Sichuan region prior to the 12 May 2008 earthquake, *Int. J. Remote Sens.* **31**, 13, 3615-3629, DOI: 10.1080/01431161003727754.

Błęcki, J., M. Parrot, and R. Wronowski (2011), Plasma turbulence in the ionosphere prior to earthquakes, some remarks on the DEMETER registrations, *J. Asian Earth Sci.* **41**, 4-5, 450-458, DOI: 10.1016/j.jseaes.2010.05.016.

Boeck, W.L., O.H. Vaughan, R.J. Blakeslee, B. Vonnegut, and M. Brook (1998), The role of the space shuttle videotapes in the discovery of sprites, jets and elves, *J. Atmos. Sol.-Terr. Phys.* **60**, 7-9, 669-677, DOI: 10.1016/S1364-6826(98)00025-X.

Claesson, L., A. Skelton, C. Graham, C. Dietl, M. Mörth, P. Torssander, and I. Kockum (2004), Hydrogeochemical changes before and after a major earthquake, *Geology* **32**, 8, 641-644, DOI: 10.1130/G20542.1.

Dea, J.Y., P.M. Hansen, and W.-M. Boerner (1997), ULF/ELF polarimetry: observations of anomalous ULF signals preceding the Northridge earthquake of January 17, 1994. **In:** H. Mott, and W.-M. Boerner (eds.), *Proc. SPIE 3120, Wideband Interferometric Sensing and Imaging Polarimetry, 27 July 1997, San Diego, USA*, DOI: 10.1117/12.300623.

Derr, J.S., F. St-Laurent, F.T. Freund, and R. Thériault (2011), Earthquake lights. **In:** H.K. Gupta (ed.), *Encyclopedia of Solid Earth Geophysics*, Springer, Dordrecht, 165-167.

Dunajecka, M.A., and S.A. Pulinets (2005), Atmospheric and thermal anomalies observed around the time of strong earthquakes in México, *Atmósfera* **18**, 236-247.

e-PISCO (2012), http://www.e-pisco.jp/index.html.

Eftaxias, K., L. Athanasopoulou, G. Balasis, M. Kalimeri, S. Nikolopoulos, and Y. Contoyiannis, J. Kopanas, G. Antonopoulos, and C. Nomicos (2009), Unfolding the procedure of characterizing recorded ultra low frequency, kHZ and MHz electromagnetic anomalies prior to the L'Aquila earthquake as pre-seismic ones – Part I, *Nat. Hazards Earth Syst. Sci*. **9**, 6, 1953-1971, DOI: 10.5194/nhess-9-1953-2009.

Filizzola, C., N. Pergola, C. Pietrapertosa, and V. Tramutoli (2004), Robust satellite techniques for seismically active areas monitoring: a sensitivity analysis on September 7, 1999 Athens's earthquake, *Phys. Chem. Earth* **29**, 4-9, 517-527, DOI: 10.1016/j.pce.2003.11.019.

Fraser-Smith, A.C. (1992), ULF, ELF, and VLF electromagnetic field observations during earthquakes: Search for precursors. **In:** S.K. Park, M.J.S. Johnston, T.R. Madden, F.D. Morgan, and H.F. Morrison (eds.), *Low Frequency Electrical Precursors: Fact or Fiction?, NSF National Earthquake Hazard Reduction Program, 14-17 June 1992, Lake Arrowhead, CA, USA*.

Freund, F. (2002), Charge generation and propagation in igneous rocks, *J. Geodyn.* **33**, 4-5, 545-570, DOI: 10.1016/S0264-3707(02)00015-7.

Freund, F.T. (2010), Toward a unified solid state theory for pre-earthquake signals, *Acta Geophys.* **58**, 5, 719-766, DOI: 10.2478/s11600-009-0066-x.

Freund, F., and S. Pilorz (2012), Electric currents in the Earth crust and the generation of pre-earthquake ULF signals. **In:** M. Hayakawa (ed.), *The Frontier of Earthquake Prediction Studies*, Nihon-senmontosho Shuppan, Tokyo, 800 pp.

Freund, F., and H. Wengeler (1982), The infrared spectrum of OH-compensated defect sites in C-doped MgO and CaO single crystals, *J. Phys. Chem. Solids* **43**, 2, 129-145, DOI: 10.1016/0022-3697(82)90131-7.

Freund, F., M.M. Masuda, and M.M. Freund (1991), Highly mobile oxygen hole-type charge carriers in fused silica, *J. Mater. Res*. **6**, 8, 1619-1622, DOI: 10.1557/JMR.1991.1619.

Freund, F.T., A. Takeuchi, and B.W.S. Lau (2006), Electric currents streaming out of stressed igneous rocks – A step towards understanding pre-earthquake low frequency EM emissions, *Phys. Chem. Earth* **31**, 4-9, 389-396, DOI: 10.1016/j.pce.2006.02.027.

Freund, F.T., A. Takeuchi, B.W.S. Lau, A. Al-Manaseer, C.C. Fu, N.A. Bryant, and D. Ouzounov (2007), Stimulated infrared emission from rocks: assessing a stress indicator, *eEarth* **2**, 1, 7-16, DOI: 10.5194/ee-2-7-2007.

Freund, F.T., I.G. Kulahci, G. Cyr, J. Ling, M. Winnick, J. Tregloan-Reed, and M.M. Freund (2009), Air ionization at rock surfaces and pre-earthquake signals, *J. Atmos. Sol.-Terr. Phys*. **71**, 17-18, 1824-1834, DOI: 10.1016/j.jastp.2009.07.013.

Freund, M.M., F. Freund, and F. Batllo (1989), Highly mobile oxygen holes in magnesium oxide, *Phys. Rev. Lett.* **63**, 19, 2096-2099, DOI: 10.1103/PhysRevLett.63.2096.

Fukuchi, T. (1996), A mechanism of the formation of E' and peroxy centers in natural deformed quartz, *Appl. Radiat. Isotopes* **47**, 11-12, 1509-1521, DOI: 10.1016/S0969-8043(96)00144-3.

Gish, O.H., and G.R. Wait (1950), Thunderstorms and the Earth's general electrification, *J. Geophys. Res*. **55**, 4, 473-484, DOI: 10.1029/JZ055i004p00473.

Gołkowski, M., M. Cohen, and M. Kubicki (2009), Global lightning activity and the atmospheric electric field. **In:** *IHY Workshop on Advancing VLF through the Global AWESOME Network*, *Tunis*.

Grant, R.A., T. Halliday, W.P. Balderer, F. Leuenberger, M. Newcomer, G. Cyr, and F.T. Freund (2011), Ground water chemistry changes before major earthquakes and possible effects on animals, *Int. J. Environ. Res. Public Health* **8**, 6, 1936-1956, DOI: 10.3390/ijerph8061936.

Gringel, W., J.M. Rosen, and D.J. Hofmann (1986), Electrical structure from 0 to 30 kilometers. **In:** *The Earth's Electrical Environment*, Studies in Geophysics, National Academy Press, Washington, D.C., 166-182.

Griscom, D.L. (1990), Electron spin resonance. **In:** D.R. Uhlmann and N.J. Kreidl (eds.), *Glass Science and Technology*, Vol. 4, Advances in Structural Analysis, 151-251, DOI: 10.1016/B978-0-12-706707-0.50010-4.

Guo, G., and B. Wang (2008), Cloud anomaly before Iran earthquake, *Int. J. Remote Sens.* **29**, 7, 1921-1928, DOI: 10.1080/01431160701373762.

Harrison, R.G., and A.J. Bennett (2007), Cosmic ray and air conductivity profiles retrieved from early twentieth century balloon soundings of the lower troposphere, *J. Atmos. Sol.-Terr. Phys*. **69**, 4-5, 515-527, DOI: 10.1016/j.jastp.2006.09.008.

Harrison, R.G., K.L. Aplin, and M.J. Rycroft (2010), Atmospheric electricity coupling between earthquake regions and the ionosphere, *J. Atmos. Sol.-Terr. Phys.* **72**, 5-6, 376-381, DOI: 10.1016/j.jastp.2009.12.004.

Hayakawa, M., Y. Kasahara, T. Nakamura, Y. Hobara, A. Rozhnoi, M. Solovieva, and O.A. Molchanov (2010), On the correlation between ionospheric perturbations as detected by subionospheric VLF/LF signals and earthquakes as characterized by seismic intensity, *J. Atmos. Sol.-Terr. Phys.* **72**, 13, 982-987, DOI: 10.1016/j.jastp.2010.05.009.

Hayakawa, M., Y. Kasahara, T. Endoh, Y. Hobara, and S. Asai (2012), The observation of Doppler shifts of subionospheric LF signal in possible association with earthquakes, *J. Geophys. Res*. **117**, A9, A09304, DOI: 10.1029/2012JA017752.

Hedge, A., and E. Eleftherakis (1982), Air ionization: An evaluation of its physiological and psychological effects, *Ann. Occup. Hyg*. **25**, 4, 409-419, DOI: 10.1093/annhyg/25.4.409.

Hollerman, W.A., B.L. Lau, R.J. Moore, C.A. Malespin, N.P. Bergeron, F.T. Freund, and P.J. Wasilewski (2006), Electric currents in granite and gabbro generated by impacts up to 1 km/s. **In:** *American Geophysical*

Union, Fall Meeting 2006, Abstract #T31A-0419, AGU, San Francisco, USA.

Hoppel, W.A., R.V. Anderson, and J.C.Willet (1986), Atmospheric electricity in the planetary boundary layer. **In:** *The Earth's Electrical Environment*, Studies in Geophysics, National Academy Press, Washington, D.C., 149-165.

İnan, S., T. Akgül, C. Seyis, R. Saatçılar, S. Baykut, S. Ergintav, and M. Baş (2008), Geochemical monitoring in the Marmara region (NW Turkey): A search for precursors of seismic activity, *J. Geophys. Res*. **113**, B3, B03401, DOI: 10.1029/2007JB005206.

İnan, S., K. Ertekin, C. Seyis, Ş. Şimşek, F. Kulak, A. Dikbaş, O. Tan, S. Ergintav, R. Çakmak, A. Yörük, M. Çergel, H. Yakan, H. Karakuş, R. Saatçilar, Z. Akçiğ, Y. Iravul, and B. Tüzel (2010), Multi-disciplinary earthquake researches in Western Turkey: Hints to select sites to study geochemical transients associated to seismicity, *Acta Geophys*. **58**, 5, 767-813, DOI: 10.2478/s11600-010-0016-7.

İnan, S., W.P. Balderer, F. Leuenberger-West, H. Yakan, A. UOzvan, and F.T. Freund (2012), Springwater chemical anomalies prior to the *Mw* = 7.2 Van earthquake (Turkey), *Geochem. J*. **46**, e11-e16.

Jhuang, H.-K., Y.-Y. Ho, Y. Kakinami, J.-Y. Liu, K.-I. Oyama, M. Parrot, K. Hattori, M. Nishihashi, and D. Zhang (2010), Seismo-ionospheric anomalies of the GPS-TEC appear before the 12 May 2008 magnitude 8.0 Wenchuan earthquake, *Int. J. Remote Sens.* **31**, 13, 3579-3587, DOI: 10.1080/01431161003727796.

Kafatos, M., D. Ouzounov, S. Pulinets, K. Hattori, J.-Y. Liu, M. Parrot, and P. Taylor (2010), Multi sensor approach of validating atmospheric signals associated with major earthquakes. **In:** *EGU General Assembly, 2-7 May 2010, Vienna, Austria*, 14184.

Kamsali, N., S.D. Pawar, P. Murugavel, and V. Gopalakrishnan (2011), Estimation of small ion concentration near the Earth's surface, *J. Atmos. Sol.-Terr. Phys.* **73**, 16, 2345-2351, DOI: 10.1016/j.jastp.2011.07.011.

Kathrein, H., and F. Freund (1983), Electrical conductivity of magnesium oxide single crystal below 1200 K, *J. Phys. Chem. Solids* **44**, 3, 177-186, DOI: 10.1016/0022-3697(83)90052-5.

King, B.V., and F. Freund (1984), Surface charges and subsurface space-charge distribution in magnesium oxides containing dissolved traces of water, *Phys. Rev. B* **29**, 10, 5814-5824, DOI: 10.1103/PhysRevB.29.5814.

Krueger, A.P., and E.J. Reed (1976), Biological impact of small air ions, *Science* **193**, 4259, 1209-1213, DOI: 10.1126/science.959834.

Krueger, A.P., P.C. Andriese, and S. Kotaka (1968), Small air ions: Their effect on blood levels of serotonin in terms of modern physical theory, *Int. J. Biometeorol.* **12**, 3, 225-239, DOI: 10.1007/BF01553423.

Kubicki, M. (2011), Global lightning activity and the atmospheric electric field. **In:** U. Inan (ed.), *The Stanford AWESOME Global Collaborative*.

Kuo, C.L. (2012), The middle atmosphere: Discharge phenomena. **In:** R. Ghadawala (ed.), *Advances in Spacecraft Systems and Orbit Determination*, InTech, Shanghai.

Kuo, C.L., J.D. Huba, G. Joyce, and L.C. Lee (2011), Ionosphere plasma bubbles and density variations induced by pre-earthquake rock currents and associated surface charges, *J. Geophys. Res*. **116**, A10, A10317, DOI: 10.1029/2011JA016628.

Linde-Gas Co. (1995), Material Safety Data Sheet: Compressed Air; www.orcbs.msu.edu/msds/LINDE_MSDS/pdf/002.pdf.

Liu, J.Y., Y.J. Chuo, S.J. Shan, Y.B. Tsai, Y.I. Chen, S.A. Pulinets, and S.B. Yu (2004), Pre-earthquake ionospheric anomalies registered by continuous GPS TEC measurements, *Ann. Geophys.* **22**, 5, 1585-1593, DOI: 10.5194/angeo-22-1585-2004.

Liu, J.Y., C.H. Chen, Y.I. Chen, W.H. Yang, K.I. Oyama, and K.W. Kuo (2010), A statistical study of ionospheric earthquake precursors monitored by using equatorial ionization anomaly of GPS TEC in Taiwan during 2001-2007, *J. Asian Earth Sci.* **39**, 1-2, 76-80, DOI: 10.1016/j.jseaes.2010.02.012.

Liu, J.Y., H. Le, Y.I. Chen, C.H. Chen, L. Liu, W. Wan, Y.Z. Su, Y.Y. Sun, C.H. Lin, and M.Q. Chen (2011), Observations and simulations of seismoionospheric GPS total electron content anomalies before the 12 January 2010 *M7* Haiti earthquake, *J. Geophys. Res*. **116**, A4, A04302, DOI: 10.1029/2010JA015704.

Liu, Y.Z., and Y. Liu (1997), The factors and mechanisms of the electromagnetics of rock fracturing, *Acta Seismol. Sinica* **19**, 4, 418-425.

Marfunin, A.S. (1979), *Spectroscopy, Luminescence, and Radiation Centers in Minerals*, Springer Verlag, Berlin.

Martens, R., H. Gentsch, and F. Freund (1976), Hydrogen release during the thermal decomposition of magnesium hydroxide to magnesium oxide, *J. Catalysis* **44**, 3, 366-372, DOI: 10.1016/0021-9517(76)90413-9.

Masci, F. (2011), On the seismogenic increase of the ratio of the ULF geomagnetic field components, *Phys. Earth Planet. In*. **187**, 1-2, 19-32, DOI: 10.1016/j.pepi.2011.05.001.

Molchanov, O.A., and M. Hayakawa (1998), On the generation mechanism of ULF seimogenic electromagnetic emissions, *Phys. Earth Planet. In.* **105**, 3-4, 201-210, DOI: 10.1016/S0031-9201(97)00091-5.

Morton, L.L. (1988), Headaches prior to earthquakes, *Int. J. Biometeorol*. **32**, 2, 147-148, DOI: 10.1007/BF01044909.

Moura, C.L., A.C. Artur, D.M. Bonotto, S. Guedes, and C.D. Martinelli (2011), Natural radioactivity and radon exhalation rate in Brazilian igneous rocks, *Appl. Radiat. Isotopes* **69**, 7, 1094-1099, DOI: 10.1016/j.apradiso.2011.03.004.

Nagaraja, K., B.S.N. Prasad, M.S. Madhava, M.S. Chandrashekara, L. Paramesh, J. Sannappa, S.D. Pawar, P. Murugavel, and A.K. Kamra (2003), Radon and its short-lived progeny: variations near the ground, *Radiat. Meas.* **36**, 1-6, 413-417, DOI: 10.1016/S1350-4487(03)00162-8.

Namgaladze, A.A., O.V. Zolotov, M.I. Karpov, and Y.V. Romanovskaya (2012), Manifestations of the earthquake preparations in the ionosphere total electron content variations, *Nat. Sci.* **4**, 11, 848-855, DOI: 10.4236/ns.2012.411113.

Ohta, K., K. Umeda, N. Watanabe, and M. Hayakawa (2001), ULF/ELF emissions observed in Japan, possibly associated with the Chi-Chi earthquake in Taiwan, *Nat. Hazards Earth Syst. Sci*. **1**, 1/2, 37-42, DOI: 10.5194/nhess-1-37-2001.

Omori, Y., H. Nagahama, Y. Kawada, Y. Yasuoka, T. Ishikawa, S. Tokonami, and M. Shinogi (2009), Preseismic alteration of atmospheric electric conditions due to anomalous radon emanation, *Phys. Chem. Earth* **34**, 6-7, 435-440, DOI: 10.1016/j.pce.2008.08.001.

Ondoh, T. (2003), Anomalous sporadic-*E* layers observed before M 7.2 Hyogo-ken Nanbu earthquake; Terrestrial gas emanation model, *Adv. Polar Upper Atmos. Res*. **17**, 96-108.

Ouzounov, D., N. Bryant, T. Logan, S. Pulinets, and P. Taylor (2006), Satellite thermal IR phenomena associated with some of the major earthquakes in 1999-2003, *Phys. Chem. Earth* **31**, 4-9, 154-163, DOI: 10.1016/j.pce.2006.02.036.

Ouzounov, D., D. Liu, K. Chunli, G. Cervone, M. Kafatos, and P. Taylor (2007), Outgoing long wave radiation variability from IR satellite data prior to major earthquakes, *Tectonophysics* **431**, 1-4, 211-220, DOI: 10.1016/j.tecto.2006.05.042.

Ouzounov, D., S. Pulinets, A. Romanov, A. Romanov, K. Tsybulya, D. Davidenko, M. Kafatos, and P. Taylor (2011), Atmosphere-ionosphere response to the M9 Tohoku earthquake revealed by joined satellite and ground observations. Preliminary results, arXiv.org, arXiv:1105.2841.

Pasko, V.P. (2006), Theoretical modeling of sprites and jets. **In:** M. Füllekrug, E.A. Mareev, and M.J. Rycroft (eds.), *Sprites, Elves and Intense Lightning Discharges*, Springer, Berlin, 253-311, DOI: 10.1007/1-4020-4629-4_12.

Pérez, N.M., P.A. Hernández, G. Igarashi, I. Trujillo, S. Nakai, H. Sumino, and H. Wakita (2008), Searching and detecting earthquake geochemical precursors in CO_2-rich groundwaters from Galicia, Spain, *Geochem. J.* **42**, 1, 75-83, DOI: 10.2343/geochemj.42.75.

Pulinets, S.A. (2007), Natural radioactivity, earthquakes, and the ionosphere, *Eos Trans. Am. Geophys. Union* **88**, 20, 217-218, DOI: 10.1029/2007EO200001.

Pulinets, S., and D. Ouzounov (2011), Lithosphere-Atmosphere-Ionosphere Coupling (LAIC) model – An unified concept for earthquake precursors

validation, *J. Asian Earth Sci.* **41**, 4-5, 371-382, DOI: 10.1016/j.jseaes.2010.03.005.

Pulinets, S.A., A. Leyva Contreras, G. Bisiacchi-Giraldi, and L. Ciraolo (2005), Total electron content variations in the ionosphere before the Colima, Mexico, earthquake of 21 January 2003, *Geofis. Int.* **44**, 4, 369-377.

Qin, K., L.X. Wu, A. De Santis, and G. Cianchini (2012), Preliminary analysis of surface temperature anomalies that preceded the two major Emilia 2012 earthquakes (Italy), *Ann. Geophys*. **55**, 4, 823-828, DOI: 10.4401/ag-6123.

Ricci, D., G. Pacchioni, M.A. Szymanski, A.L. Shluger, and A.M. Stoneham (2001), Modeling disorder in amorphous silica with embedded clusters: The peroxy bridge defect center, *Phys. Rev. B* **64**, 22, 224101-224108, DOI: 10.1103/PhysRevB.64.224104.

Roberts, L., and F. Freund (2012), Coupling between Earth surface and ionosphere before earthquakes air ionization at the ground-to-air interface as major driving mechanism. **In:** T. Nagao (ed.), *EMSEV 2012 Workshop, 1-4 October 2012, Gotemba, Japan*.

Rycroft, M.J., S. Israelsson, and C. Price (2000), The global atmospheric electric circuit, solar activity and climate change, *J. Atmos. Sol.-Terr. Phys*. **62**, 17-18, 1563-1576, DOI: 10.1016/S1364-6826(00)00112-7.

Rycroft, M.J., A. Odzimek, N.F. Arnold, M. Füllekrug, A. Kułak, and T. Neubert (2007), New model simulations of the global atmospheric electric circuit driven by thunderstorms and electrified shower clouds: The roles of lightning and sprites, *J. Atmos. Sol.-Terr. Phys*. **69**, 17-18, 2485-2509, DOI: 10.1016/j.jastp.2007.09.004.

Rycroft, M.J., R.G. Harrison, K.A. Nicoll, and E.A. Mareev (2008), An overview of Earth's global electric circuit and atmospheric conductivity, *Space Sci. Rev*. **137**, 1-4, 83-105, DOI: 10.1007/s11214-008-9368-6.

Sapkota, B.K., and N.C. Varshneya (1990), On the global atmospheric electrical circuit, *J. Atmos. Terr. Phys*. **52**, 1, 1-20, DOI: 10.1016/0021-9169(90)90110-9.

Saraf, A.K., V. Rawat, P. Banerjee, S. Choudhury, S.K. Panda, S. Dasgupta, and J.D. Das (2008), Satellite detection of earthquake thermal infrared precursors in Iran, *Nat. Hazards* **47**, 1, 119-135, DOI: 10.1007/s11069-007-9201-7.

Saraf, A.K., V. Rawat, J. Das, M. Zia, and K. Sharma (2012), Satellite detection of thermal precursors of Yamnotri, Ravar and Dalbandin earthquakes, *Nat. Hazards* **61**, 2, 861-872, DOI: 10.1007/s11069-011-9922-5.

Shitov, A.V. (2010), Health of people living in a seismically active region. **In:** I. Florinsky (ed.), *Man and the Geosphere*, Nova Science Publishers, Inc., New York, 185-214.

Shluger, A.L., E.N. Heifets, J.D. Gale, and C.R.A. Catlow (1992), Theoretical simulation of localized holes in MgO, *J. Phys. – Condens. Mat.* **4**, 26, 5711-5722, DOI: 10.1088/0953-8984/4/26/005.

Singh, A.K., D. Siingh, R.P. Singh, and S. Mishra (2011), Electrodynamical coupling of Earth's atmosphere and ionosphere: An overview, *Int. J. Geophys*. **2011**, 971313, DOI: 10.1155/2011/971302.

Sorokin, V.M., V.M. Chmyrev, and A.K. Yaschenko (2005), Theoretical model of DC electric field formation in the ionosphere stimulated by seismic activity, *J. Atmos. Sol.-Terr. Phys*. **67**, 14, 1259-1268, DOI: 10.1016/j.jastp.2005. 07.013.

Thomas, J.N., J.J. Love, and M.J.S. Johnston (2009), On the reported magnetic precursor of the 1989 Loma Prieta earthquake, *Phys. Earth Planet. In.* **173**, 3-4, 207-215, DOI: 10.1016/j.pepi.2008.11.014.

Tramutoli, V., V. Cuomo, C. Filizzola, N. Pergola, and C. Pietrapertosa (2005), Assessing the potential of thermal infrared satellite surveys for monitoring seismically active areas: The case of Kocaeli (İzmit) earthquake, August 17, 1999, *Remote Sens. Environ*. **96**, 3-4, 409-426, DOI: 10.1016/j.rse. 2005.04.006.

Tronin, A.A. (1996), Satellite thermal survey – a new tool for the study of seismoactive regions, *Int. J. Remote Sens.* **17**, 8, 1439-1455, DOI: 10.1080/ 01431169608948716.

Vallianatos, F., and D. Triantis (2008), Scaling in pressure stimulated currents related with rock fracture, *Physica A* **387**, 19-20, 4940-4946, DOI: 10.1016/ j.physa.2008.03.028.

Walker, S.N., M.A. Balikhin, O.A. Pokhotelov, and M. Parrott (2012), DEMETER ULF observations of turbulence during the period before large earthquakes. **In:** *EGU General Assembly, 22-27 April 2012, Vienna, Austria*, 5827.

Yoshida, S., and T. Ogawa (2004), Electromagnetic emissions from dry and wet granite associated with acoustic emissions, *J. Geophys. Res*. **109**, B9, DOI: 10.1029/2004JB003092.

Received 8 August 2012
Received in revised form 19 January 2013
Accepted 25 January 2013